Desalination and Water Treatment
www.deswater.com

doi: 10.1080/19443994.2013.769659

51 (2013) 5664–5673
August

Taylor & Francis
Taylor & Francis Group

An adsorption diffusion model for removal of copper (II) from aqueous solution by pyrolytic tyre char

Ali Shahtalebi[a,b], Mohammad Hossein Sarrafzadeh[a,*], Gordon McKay[b]

[a]*School of Chemical Engineering, College of Engineering, University of Tehran, Tehran, Iran*
Tel. +982161112185; Fax: +982166957784; email: sarrafzdh@ut.ac.ir
[b]*Department of Chemical Engineering, Hong Kong University of Science and Technology, Hong Kong, P.R. China*

Received 11 August 2011; Accepted 10 December 2012

ABSTRACT

Kinetic and equilibrium adsorption experiments have been carried out in order to investigate the removal and diffusion mechanism of copper (II) ions onto pyrolytic tyre char obtained from an industrial plant. The experimental equilibrium data have been analyzed using Langmuir, Freundlich, and Redlich–Peterson isotherm models. The accuracy of the fit of the isotherm models to experimental equilibrium data was assessed using the sum of squares error (SSE) analysis. Modeling of the adsorption isotherm showed that Redlich–Peterson expression yields the best fit between experimental and predicted data. The batch kinetic data obtained at different concentrations of copper ions in the solution and also different masses of tyre char were analyzed using the intraparticle diffusion model. In the intraparticle diffusion model plots, three distinct linear sections were obtained for every batch operation. An intraparticle diffusion rate parameter, k is derived from the plots of copper adsorbed vs. the square root of time. The data indicated the potential of pyrolytic tyre char for the removal of copper from aquatic effluents and the adsorption mechanism of copper ions onto tyre char can be described by intraparticle diffusion model.

Keywords: Adsorption; Kinetic experiments; Copper; Intraparticle diffusion modeling; Tyre Char

1. Introduction

The removal of heavy metals from effluents is among the most important issues for many industrialized countries. The aqueous wastes containing heavy metals such as copper which is among the toxic pollutants in marine, ground, and industrial wastewaters are concerns of public, industry, and governments [1]. Therefore, the treatment processes for the removal of copper from water and wastewater are very important. There are several methods available to achieve the reduction of metal ions in wastewater such as chemical precipitation, membrane separation, and sorption/ion exchange [2–4]. Sorption is a more efficient and low cost process, and it is an attractive option because of the basic simplicity of the application [3,4].

The most widely studied adsorbent is activated carbon [5,6], but the application of other adsorbent materials for metal ion removal has also been investigated [7]. Beech leaves [8] and banana pith [9] have been used to adsorb copper. Other materials studied

*Corresponding author.

for copper sorption include coconut husk [10], hyacinth roots [11], palm fiber [12], and chitosan [13].

Pyrolysis has been shown to be a technically feasible method to produce activated carbon sorbents [14–17] that can be used for wastewater treatment [18,19]. However, although numerous studies have been carried out on the use of pyrolyzed tyre chars to remove hazardous chemicals, especially heavy metals from waste aqueous streams, the kinetics involved in the sorption process is not completely understood yet.

In order to optimize the design and operation of an adsorption system, it is essential to study the adsorption equilibrium and kinetics which could supply the fundamental information of adsorption. The equation parameters of the equilibrium models provide some insight into the sorption mechanism and affinity of the sorbent [20]. It is also essential to have information relating the rate of pollutant removal from the liquid phase to the various mass transfer and diffusion coefficients of the system [21]. Although various models have been used to describe the adsorption kinetics, most of them such as the homogeneous surface diffusion model, pore diffusion model and heterogeneous diffusion model (also known as pore and diffusion model) need many parameters which require lots of experiments and massive calculation time which have made them inconvenient for practical use [22–24]. Therefore, several simplified models have been developed, which could also explain the whole adsorption process for many adsorption systems [25–28]. One of the well-known kinetic models is the intraparticle diffusion model which assumes that the film diffusion is negligible and intraparticle diffusion is the only rate-controlling step [26,29].

If the adsorption process follows the intraparticle diffusion model, a plot of q_t (adsorbate uptake) against $t^{0.5}$ should be a straight line [30]. The mathematical dependence on $t^{0.5}$ is obtained, if the sorption is considered to be influenced by intraparticle diffusion in spherical particles and convective diffusion in the solution [21,31]. The intraparticle diffusion model has been used in various adsorption systems and it has been found that this model could explain the adsorption mechanism in many well-stirred adsorption systems [21,30,32].

The objective of this research is to study the adsorption mechanism of copper ions from aqueous solution onto pyrolytic tyre char and to further evaluate the validity of intraparticle diffusion model for this system. Firstly, the experimental equilibrium data has been evaluated by Langmuir, Freundlich, and Redlich–Peterson isotherm models and then, the kinetic results of the kinetic experiments are analyzed using the intraparticle diffusion model to test the mechanism and correlate the experimental data. This paper reports the effect of process variables such as initial copper concentration and mass of tyre char on the intraparticle diffusion model parameter.

2. Materials and methods

2.1. Materials

For the preparation of tyre char as an adsorbent for our experiments, the remaining steel wires were removed from the raw pyrolytic tyre char that was obtained from an industrial plant. After sieving to obtain tyre chars with particle size of 710–1,000 μm, they were then heated at 550°C under the flow of nitrogen (purity 99.99%) gas to ensure that all the remaining volatile compounds were removed. Chars were then washed until the pH of the solution becames steady. The characteristics of the tyre chars including the surface area, pore volume, and the pore size distribution have been investigated elsewhere [33].

Copper ion was considered as the adsorbate and its solutions were prepared in deionized water using copper (II) sulfate which was of analytical grade like all the chemicals used in this study. All solutions were adjusted to pH 4 using diluted nitric acid.

2.2. Equilibrium adsorption experiment

A fixed mass of tyre char (0.05 g) was weighed into 120 mL test bottles and 50 mL of copper ion solutions of different concentrations were added by pipette to make a range of copper ion concentration solutions (0.75–3.2 mmol/L) at initial pH 4.0 ± 0.1.

The solutions were sealed and agitated in the shaker bath (200 rpm shaking rate) at constant temperature 25 ± 2°C until equilibrium was reached. Each test bottle was removed from the shaker at a specified time and the copper ion solution was collected in a sample tube. To ensure that the isotherm achieved equilibrium, the agitation time was defined as 96 h in the isotherm experiment. The concentration of solute in the aqueous phase was analyzed by utilizing the Inductively Coupled Plasma Atomic Emission Spectrophotometer (ICP–AES).

The amount of copper ion adsorbed at equilibrium (q_e) was calculated by the mass balance equation, which is represented as:

$$q_e = \frac{V(C_0 - C_e)}{M} \quad (1)$$

where C_0 (mmol/L) and C_e (mmol/L) are the concentration of solute in aqueous phase at initiation and equilibrium, respectively, V (L) is the volume of the aqueous solution, and M (g) is the mass of tyre char.

2.3. Kinetic experiments

An adsorption vessel (a baffled agitated sorber vessel holding 1.7 L of copper solution) was used to obtain kinetic data and investigate the influence of initial copper concentration and mass of tyre char on the adsorption rate. The inner diameter of the adsorption tank was 0.13 m. A flat plastic impeller with six blades provided mixing effect to the solution. The diameter of the impeller was 0.065 m and the height of all the blades was 0.013 m. An overhead stirrer was used to drive the impeller using a 0.005 m diameter plastic shaft. Six plastic baffles were located around the circumference of the vessel with a position at 60° intervals and held securely in place on the top of the vessel. The baffles prevent the formation of a vortex and the consequential reduction in the relative motion between the solid and liquid. Each baffle was located slightly away from the wall of the vessel to prevent the solid accumulation. All materials in contact with solutions were made from Perspex. The relationships with respect to the inner vessel diameter (D_i) for adsorption vessel are shown in Fig. 1.

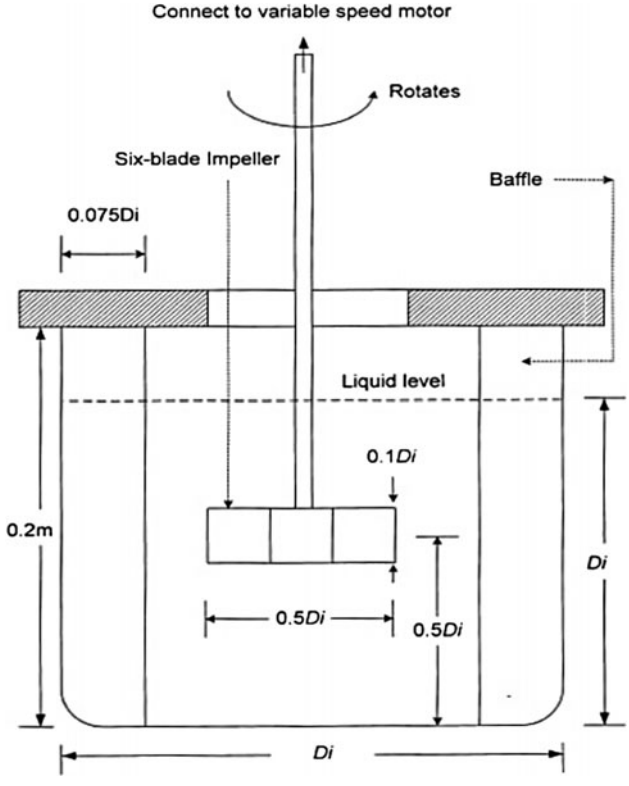

Fig. 1. Adsorption setup for batch-contact-time studies.

A fixed mass of tyre char (1.7 g) was added to each 1.7 L volume of copper (II) sulfate solution. The initial pH value of copper solutions was adjusted at 4.0 ± 0.1. An agitation speed of 400 rpm at 25 ± 2°C was used in all experiments. Different initial concentrations of copper ions (0.41, 0.63, 0.83, 1.06, and 1.24 mmol/L) were used in these series of experiments while for the effect of different mass of tyre char, the initial concentration of copper was set at 1 mmol/L and five different masses of tyre char (0.850, 1.275, 1.700, 2.125, and 3.400 g) were used.

During the experiments, 10 mL syringes were used to withdraw 5 mL samples. The samples were filtered through membrane filters before the injection into sample tubes and then analyzed by ICP–AES for all the studies.

2.4. Intraparticle diffusion modeling

Diffusional adsorption is usually controlled by an external film resistance and/or internal diffusion mass transport (intraparticle diffusion). In intraparticle diffusion modeling for well-mixed solutions, it is assumed that the film diffusion is negligible and intraparticle diffusion is the only rate-controlling step. The intraparticle diffusion model can be derived from Fick's second law under two assumptions to describe the adsorption process in terms of the $q_t - t^{0.5}$ relationship; firstly, it is assumed that intraparticle diffusivity is constant and secondly, the uptake of sorbate by the sorbent is small in comparison to the total quantity of sorbate which is present in the solution [34].

Theoretical analysis of intraparticle diffusion yields complex mathematical relationships depending on the particle shape. For adsorption onto spherical particles with a constant diffusivity, Crank [35] proposed the following equations:

$$\frac{q_t}{q_e} = 1 - \frac{6}{\pi^2}\sum\frac{1}{n^2}\exp\left(-\frac{n^2\pi^2 D_s t}{r^2}\right) \quad (2)$$

$$\frac{q_t}{q_e} = 6\left(\frac{D_s t}{r^2}\right)^{0.5}\left[\frac{1}{\sqrt{\pi}} + 2\sum \text{ierfc}\left(\frac{nr}{\sqrt{D_s t}}\right)\right] - \frac{3D_s t}{r^2} \quad (3)$$

where

$$\text{ierfc} = \int_x^\infty \text{erfc}\ \xi\, d\xi = \frac{1}{\pi^{1/2}}e^{-x^2} - x\ \text{erfc}\ x \quad (4)$$

$$\text{erf}\, x = \frac{2}{\pi^{1/2}} \int_0^x \exp(-\eta^2) d\eta \tag{5}$$

$$\eta = \xi / 2\sqrt{D_s t} \tag{6}$$

and q_e (mg/g) and q_t (mg/g) are the solid phase concentration at equilibrium and time t (min), respectively, D_s is surface diffusivity ($cm^2\ s^{-1}$), and r (cm) is radius of sorbent. In the earlier stages of the adsorption process, when t is relatively small, Eq. (3) reduces to

$$q_t = \frac{6 q_e D_s^{0.5}}{\pi^{0.5} r} t^{0.5} \tag{7}$$

which can be represented by:

$$q_t = k \times t^{0.5} \tag{8}$$

where k is defined as the intraparticle diffusion rate constant and is related to the intraparticle diffusivity in the following equation,

$$k = \frac{6 q_e}{r} \sqrt{\frac{D}{\pi}} \tag{9}$$

Eq. (8) shows that a plot of q_t (mg/g), vs. the square root of time $t^{0.5}$ would yield a straight line passing through the origin if the adsorption process obeyed the intraparticle diffusion model. The slope of the straight line equals to k, the intrapaticle diffusion rate constant.

3. Results and discussion

3.1. Adsorption isotherm study

The equilibrium isotherm for the adsorption of copper ions was measured experimentally and the experimental data were fitted to Langmuir, Freundlich, and Redlich–Peterson equations using nonlinear optimization to determine which isotherm gives the best correlation to experimental data. The experimental data and isotherm models are shown in Fig. 2.

3.1.1. Langmuir isotherm

Langmuir [36] proposed a theory to describe the adsorption of gas molecules onto metal surfaces. The Langmuir adsorption isotherm has been applied successfully in many real monolayer sorption processes. Langmuir's model predicts the existence of monolayer coverage of the adsorbate at the outer surface of the adsorbent. This isotherm equation assumes that adsorption takes place at specific homogeneous sites within the adsorbent [36,37]. This model also assumes that each site can accommodate only one molecule and all sorption sites are identical and energetically equivalent. The Langmuir model can be represented as follows:

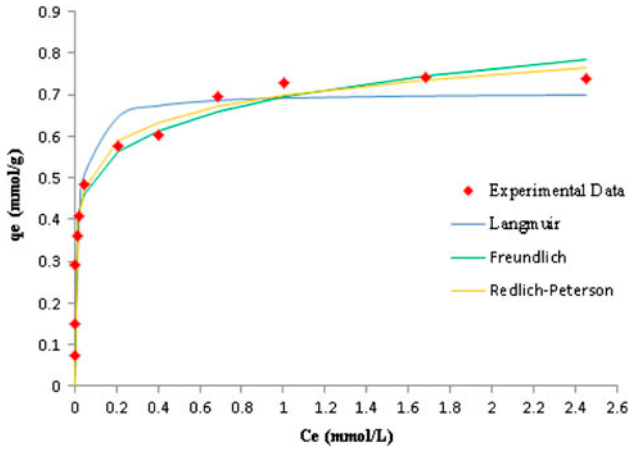

Fig. 2. Experimental equilibrium data and predicted isotherm models (Shaker speed: 200 rpm, Temp: 25 ± 2°C, pH: 4.0 ± 0.1).

$$q_e = \frac{q_m a_L C_e}{1 + a_L C_e}$$

or, alternatively

$$q_e = \frac{K_L C_e}{1 + a_L C_e} \tag{10}$$

where q_e is the solid phase sorbate concentration at equilibrium (mmol/g), C_e is the aqueous phase sorbate concentration at equilibrium (mmol/L), K_L is Langmuir isotherm constant (L/g), a_L is Langmuir isotherm constant (L/mmol). Fig. 2 shows the Langmuir model for the copper-tyre char system. The predicted isotherm parameters are also shown in Table 1.

3.1.2. Freundlich Isotherm

The most important multisite adsorption isotherm for heterogeneous surfaces is the Freundlich adsorption isotherm in which it is characterized by the heterogeneity factor $1/n$ [38]. The Freundlich equation can be written as:

$$q_e = K_F C_e^{1/n} \tag{11}$$

Table 1
Parameter values from fitting the adsorption equilibrium data with isotherm models

Equilibrium isotherms	Model parameters	SSE
Langmuir	a_L: 53.73	0.1312
	q_m: 0.71	
Freundlich	K_f: 0.69	0.1200
	$1/n$: 0.13	
	K_R: 100.89	0.1168
Redlich–Peterson	a_R: 143.46	
	β: 0.90	

where q_e is solid phase sorbate concentration in equilibrium (mmol/g), C_e is liquid phase sorbate concentration in equilibrium (mmol/L), K_F is Freundlich constant (L/g), and $1/n$ is the heterogeneity factor which is shown in Table 1.

The Freundlich isotherm is not restricted to the formation of the monolayer. The Freundlich equation predicts that the copper ion concentrations on the adsorbent will increase as there is an increase in the copper ion concentration in the liquid.

3.1.3. Redlich–Peterson isotherm

Jossens et al. [39] incorporated the features of the Langmuir and Freundlich isotherms into a single equation and presented a general isotherm equation. The mechanism of adsorption in this model, which is a three parameter model, does not follow the ideal monolayer adsorption. The Redlich–Peterson isotherm is represented as follows:

$$q_e = \frac{K_R C_e}{1 + a_R C_e^{\beta}} \tag{12}$$

where q_e is solid phase sorbate concentration in equilibrium (mmol/g), C_e is liquid phase sorbate concentration in equilibrium (mM), K_R is Redlich–Peterson isotherm constant (L/g), a_R is Redlich–Peterson isotherm constant ($mM^{-1/\beta}$), and β is the exponent which lies between 1 and 0.

In the limits, as the exponent β tends to zero, the equation becomes like Freundlich model, or heterogeneous, and as the exponent β tends to 1, the equation approaches the ideal Langmuir condition.

The isotherm parameters for these three models were determined by minimizing the distance between the experimental data points and the models' predictions. Nonlinear optimization using sum-of-squares-error (SSE) with the aid of SOLVER add-in by Microsoft Excel has been applied to determine the isotherm parameters. The SSE function is represented mathematically as follows:

$$\mathrm{SSE} = \sum \left(q_{\mathrm{exp,i}} - q_{\mathrm{cal,i}}\right)^2 \tag{13}$$

where q_{exp} is the experimental sorption capacity data and q_{cal} is the theoretical sorption kinetic model. Since the SSE method represents the square of the distance between the experimental data points and the models, the SSE value can assist in identifying the best-fit equation. Table 1 shows that the least values of SSE are given by the Redlich–Peterson model. Freundlich equation also gives lower SSE than Langmuir. The low heterogeneity factor ($1/n$) in Freundlich model suggests a highly heterogeneous surface of tyre char. The monolayer capacity (q_m) based on the Langmuir analysis is 0.71 mmol/g which reflects that tyre char has good capacity of adsorbing copper ions.

3.2. Adsorption kinetics study

Figs. 3 and 4 typically show the time profiles of liquid-phase concentrations (C_t / C_0) for adsorption of copper (II) ions onto tyre char for different concentrations of copper (II) ions and different masses of tyre char, respectively at pH 4.

The metal ion concentrations have considerable effects in the adsorption processes. The metal uptake depends on the initial metal concentration. Another important factor that strongly affects the sorption capacity is the concentration of the sorbent. Fig. 4 shows the effect of the mass of adsorbent on the removal of copper ions from the solution. In this Fig, it is clear that C_t/C_0 decreases with increasing the

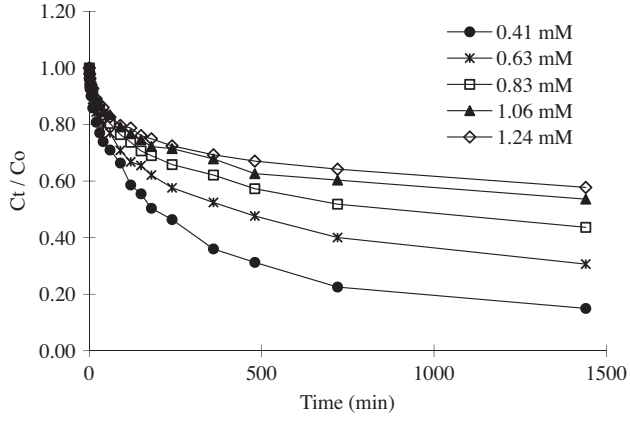

Fig. 3. Time profiles of liquid-phase concentrations of Cu (II) at different initial solute concentrations (pH: 4).

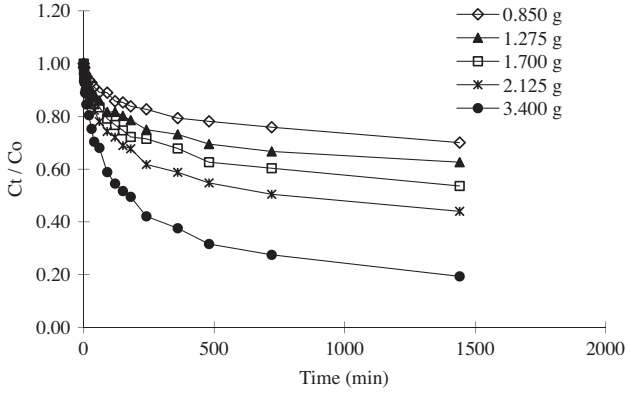

Fig. 4. Time profiles of liquid-phase concentrations of Cu (II) at different masses of sorbent (pH: 4).

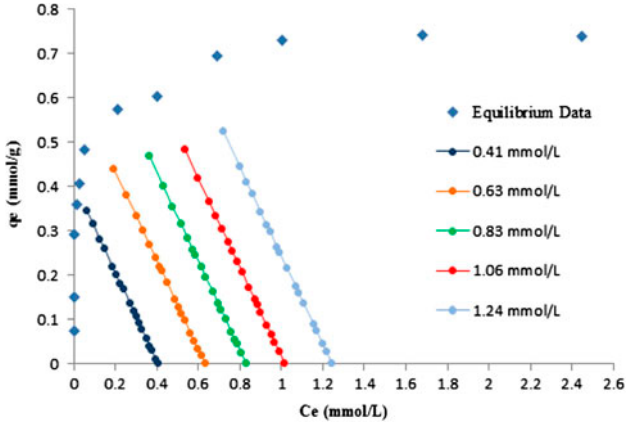

Fig. 5. Operating line plots for different concentrations of copper.

mass of adsorbent, which indicates that the adsorbate uptake decreases with increasing mass of adsorbent.

The results from the kinetic study could be linked up with the equilibrium data. Each value of C_t (from a single-batch kinetic experiment) was plotted on the isotherm and the corresponding q_t can be calculated by Eq. (1). The slope of operating lines is dependent on the ratio of V/M. The operating lines for each kinetic experiment are drawn in Figs. 5 and 6.

As can be seen by the operating line plots, the batch kinetic systems take a long time to reach equilibrium and the final C_t and q_t values have not reached the isotherm boundary line even operating the batch systems for more than 24 h. Theoretically, the values of equilibrium solid-phase concentration and equilibrium liquid-phase concentration when time equal to infinite ($C_{e,\infty}$ and $q_{e,\infty}$) can be determined by extending the operating line to the isotherm boundary line.

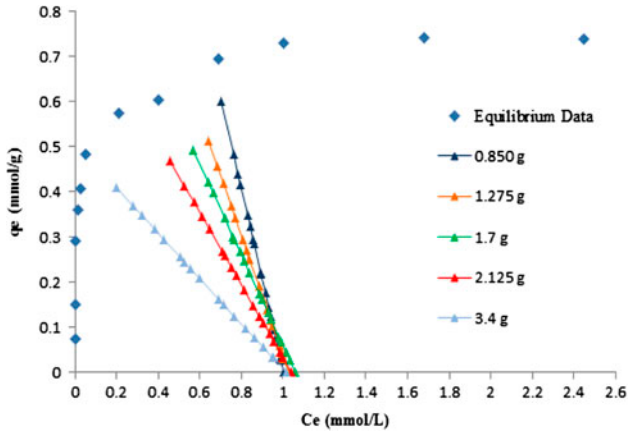

Fig. 6. Operating line plots for different masses of tyre char.

To identify the diffusion mechanism of the copper ion adsorption onto tyre char, the intraparticle diffusion model which was proposed by Weber and Morris [40] has been used. If the adsorption process follows the intraparticle diffusion model, a plot of q against $t^{0.5}$ should be a straight line. The intraparticle parameter (k_p) can be calculated from the slope of the straight line. It is common to observe multilinearity on the $q - t^{0.5}$ plot, which reveals the different stages in adsorption including external mass transfer followed by intraparticle diffusion [30]. Allen et al. [21] suggested that the multilinearity of intraparticle diffusion plots may be due to two or more steps occurring. McKay and Poots [41] identified three linear sections on the root-time plot in a dye adsorption process. The authors explained the three sections in terms of pore diameters macropores, mesopores, and micropores.

In Figs. 7 and 8, the intraparticle diffusion model plots for the copper tyre char system, under the effect of initial copper concentration and mass of tyre char are shown. It is observed that there are three linear sections elucidating three adsorption stages, which depict external mass transfer followed by intraparticle diffusion.

The model parameters, k_1, k_2, and k_3 for these three regions in the figures were determined from the slope of the lines. These parameters refer to the macropore, mesopore, and micropore diffusion parameters, respectively. Mass of copper adsorbed per unit mass of tyre char per square root of time (mmol copper g^{-1} tyre char $min^{-0.5}$) is the dimension of the intraparticle diffusion parameter. The numerical values of the rate parameters obtained from the experimental plots are presented in Table 2. This table shows that the intraparticle parameters increase with

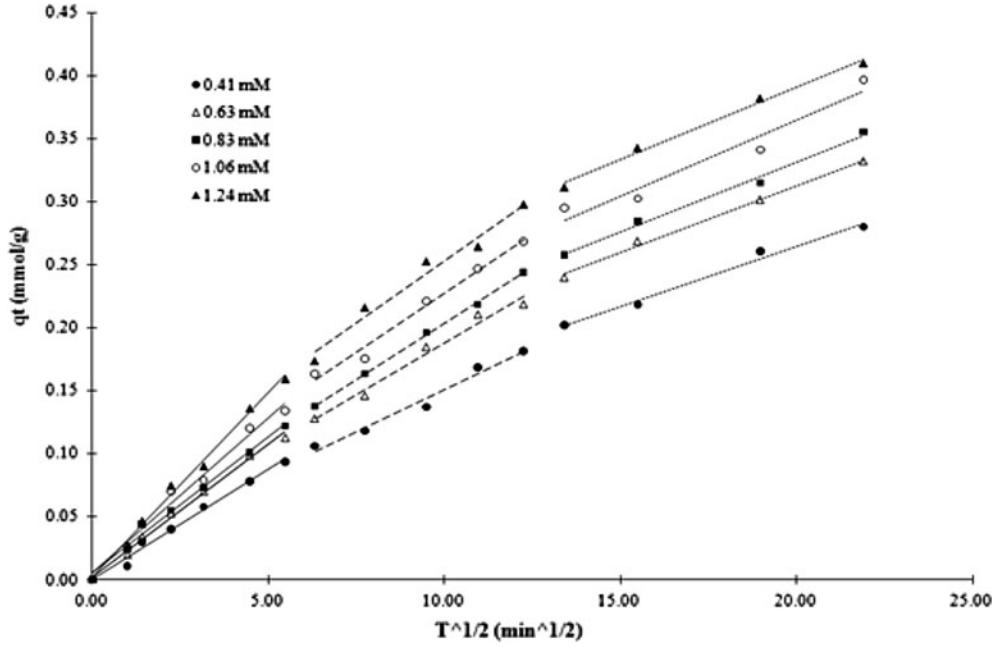

Fig. 7. Solid phase concentration against square root of time (Effect of initial copper concentration).

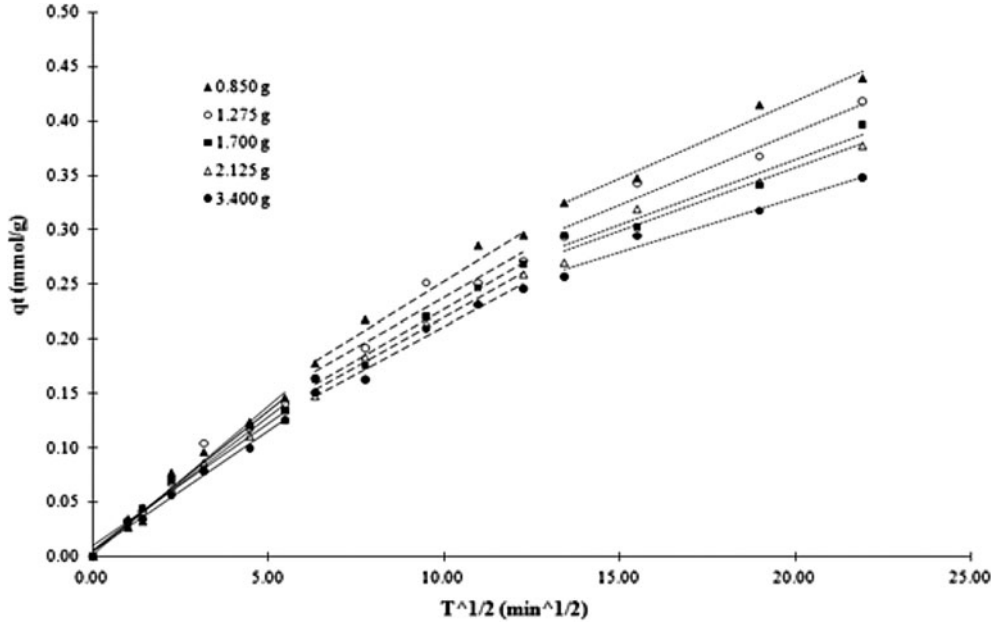

Fig. 8. Solid phase concentration against square root of time (Effect of mass of tyre char).

increasing initial copper concentration which may be because of the greater concentration gradient in the bulk solution phase and the solid phase. From Eq. (9), it also can be seen that intraparticle parameter (k) is proportional to both q_e and $D^{1/2}$. The equilibrium concentration q_e increases accordingly with increasing initial copper concentration. Some studies have reported that the intraparticle diffusion, D, increases with the increasing initial concentration [43–45]. Consequently, the constant (k) increases with increasing initial concentration due to the increasing q_e and $D^{1/2}$.

Table 2
Intraparticle rate parameters for copper-tyre char system variables

System variables	k_1 (mmol g^{-1} $min^{-0.5}$)	R^2	k_2 (mmol g^{-1} $min^{-0.5}$)	R^2	k_3 (mmol g^{-1} $min^{-0.5}$)	R^2
Effect of initial copper concentration (mM)						
0.41	0.0174	0.9884	0.0133	0.9758	0.0096	0.9867
0.63	0.0211	0.9939	0.0165	0.9784	0.0106	0.9951
0.83	0.0216	0.9897	0.0179	0.9989	0.0111	0.9923
1.06	0.0246	0.9841	0.0188	0.9843	0.0120	0.9450
1.24	0.0293	0.9937	0.0196	0.9722	0.0115	0.9920
Effect of mass of tyre char (g)						
0.850	0.0273	0.9791	0.0201	0.9223	0.0143	0.9768
1.275	0.0258	0.9754	0.0184	0.9201	0.0135	0.9586
1.700	0.0246	0.9841	0.0188	0.9843	0.0120	0.9450
2.125	0.0224	0.9778	0.0181	0.9882	0.0118	0.9463
3.400	0.0220	0.9915	0.0173	0.9737	0.0100	0.9658

The rate parameters show a decrease in value as mass of tyre char increases. The increased mass of tyre char will cause an increase in the rate of copper ions removal from the solution. This will cause a rapid decrease in copper ion concentration which results in reduction in the driving force for intraparticle diffusion.

The rate parameters could be correlated against each system variable (concentration of copper ions or mass of tyre char) by:

$$K_i = A_i(variable)^{B_i} \quad (14)$$

or

$$\log k_i = \log A_i + B_i \log(variable) \quad (15)$$

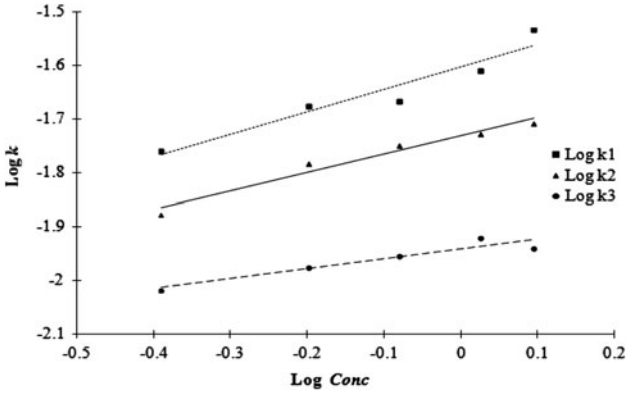

Fig. 9. Log k against log concentration.

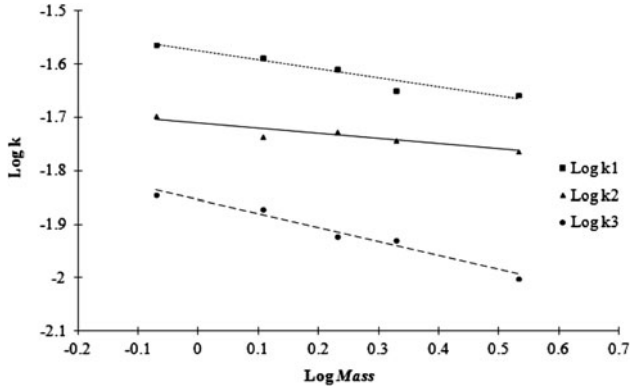

Fig. 10. Log k against log mass.

where A_i and B_i are the correlation constants and the *variable* can be initial copper concentration or mass of tyre char, k_i ($i = 1$–3) represents the model parameter. The plots of log k vs. log *variable* are presented in Figs. 9 and 10. The values of the intraparticle rate parameters, which were obtained from the slope of the q_t vs. $t^{0.5}$ plots, are summarized in Table 3.

As can be seen, the rate parameters vary with the change of the system variable in different extent. In the initial stage of copper adsorption onto tyre char, with the large concentration gradient, the diffusion rate constant is the largest. It can be seen that the rate parameters for the diffusion in bigger pores are higher than those for the smaller pores. This is related to the available free path for diffusion in the type of pore size. There is the possibility of pore blockage or steric hindrance exerted by the adsorbed molecules on the tyre char surface and it will eventually slow down the adsorption process.

Table 3
Correlation values for the effect of process variables

Variable	k_1		k_2		k_3	
	A_1	B_1	A_2	B_2	A_3	B_3
Initial copper concentration	0.0250	0.4199	0.0186	0.3407	0.0114	0.1843
Mass of tyre char	0.0266	−0.1692	0.0195	−0.0981	0.0140	−0.2602

4. Conclusions

The adsorption equilibrium and kinetics of copper ions onto tyre char have been studied in the present work. The equilibrium data were evaluated by the Langmuir, Freundlich, and Redlich–Peterson isotherm models—of which the Redlich–Peterson model yields the best fit between experimental and predicted data. The relatively high sorption capacity indicates that tyre char can be considered as a suitable sorbent for the adsorption of copper in wastewater treatment systems. The adsorption kinetic data was also investigated by the intraparticle diffusion model under the effects of initial copper concentration and mass of tyre char. Analysis of mechanism reveals that the adsorption process of copper ions onto tyre char includes three stages. The adsorption processes were related to a possible pore size distribution by obtaining distinct linear sections in the intraparticle plots with different rate constants (slope values), which show the existence of three adsorption stages with variable adsorption rates. The intraparticle rate parameters indicate that the sorption rate at longer time periods is reduced. It was suggested that the lower rates of adsorption could be related to the pore structure of the tyre char.

Acknowledgments

Authors would like to thank Prof. Jang K. Kim for providing such a fruitful collaboration between Hong Kong UST and University of Tehran.

References

[1] K. Chong, B. Volesky, Metal biosorption equilibria in a ternary system, Biotech. and Bioeng. 49(6) (1996) 629–638.
[2] A. El-Kamash, A. Zaki, M.A. El Geleel, Modeling batch kinetics and thermodynamics of zinc and cadmium ions removal from waste solutions using synthetic zeolite A, J. Hazard. Mater. 127(1) (2005) 211–220.
[3] W. Cheung, J. Ng, G. Mckay, Kinetic analysis of the sorption of copper (II) ions on chitosan, J. Chem. Technol. Biotechnol. 78(5) (2003) 562–571.
[4] S. Svilović, D. Rušić, R. Stipišić, Modeling batch kinetics of copper ions sorption using synthetic zeolite NaX, J. Hazard. Mater. 170(2) (2009) 941–947.
[5] G. McKay, M.J. Bino, Adsorption of pollutants on to activated carbon in fixed beds, J. Chem. Technol. Biotechnol. 37(2) (1987) 81–93.
[6] A. Netzer, D. Hughes, Adsorption of copper, lead and cobalt by activated carbon, Water Res. 18(8) (1984) 927–933.
[7] C.F. Forster, D.A.J. Wase, Biosorbents for Metal Ions, Taylor & Francis Publication, London, 1997.
[8] R. Salim, M. Al-Subu, E. Sahrhage, Uptake of beech leaves cadmium from water by beech leaves, J. Environ. Sci. Health Part A 27(3) (1992) 603–627.
[9] C. Lee, K. Low, K. Kek, Removal of chromium from aqueous solution, Bioresour. Technol. 54(2) (1995) 183–189.
[10] K. Low, C. Lee, K. Tan, Biosorption of basic dyes by water hyacinth roots, Bioresour. Technol. 52(1) (1995) 79–83.
[11] K. Low, C. Lee, C. Tai, Biosorption of copper by water hyacinth roots, J. Envir. Sci. Health Part A 29(1) (1994) 171–188.
[12] K. Low, C. Lee, K. Lee, Sorption of copper by dye-treated oil-palm fibres, Bioresour. Technol. 44(2) (1993) 109–112.
[13] A. Findon, G. McKay, H.S. Blair, Transport studies for the sorption of copper ions by chitosan, J. Environ. Sci. Health Part A 28(1) (1993) 173–185.
[14] A. Quek, X.S. Zhao, R. Balasubramanian, Mechanistic insights into copper removal by pyrolytic tire char through equilibrium studies, Ind. Eng. Chem. Res. 49(10) (2010) 4528–4534.
[15] A. Quek, R. Balasubramanian, Removal of copper by oxygenated pyrolytic tire char: Kinetics and mechanistic insights, J. Colloid Interface Sci. 356(1) (2011) 203–210.
[16] E.L.K. Mui, D.C.K. Ko, G. McKay, Production of active carbons from waste tyres—A review, Carbon 42(14) (2004) 2789–2805.
[17] D.C.K. Ko, E.L.K. Mui, K.S.T. Lau, G. McKay, Production of activated carbons from waste tire–process design and economical analysis, Waste Manage. (Oxford) 24(9) (2004) 875–888.
[18] N.K. Hamadi, X.D. Chen, M.M. Farid, M.G.Q. Lu, Adsorption kinetics for the removal of chromium (VI) from aqueous solution by adsorbents derived from used tyres and sawdust, Chem. Eng. J. 84(2) (2001) 95–105.
[19] P.Y. Chang, Y.L. Wei, Y.W. Yang, J.F. Lee, Removal of copper from water by activated carbon, Bull. Environ. Contam. and Toxicol. 71(4) (2003) 791–797.
[20] Y. Ho, J. Porter, G. McKay, Equilibrium isotherm studies for the sorption of divalent metal ions onto peat: Copper, nickel and lead single component systems, Water Air Soil Pollut. 141(1) (2002) 1–33.
[21] S. Allen, G. McKay, K. Khader, Intraparticle diffusion of a basic dye during adsorption onto sphagnum peat, Environ. Pollut. 56(1) (1989) 39–50.
[22] Y. Ho, G. McKay, A comparison of chemisorption kinetic models applied to pollutant removal on various sorbents, Process safety and Environmental Protection: Transactions of the Institution of Chemical Engineers, part B 76(4) (1998) 332–340.
[23] E. Guibal, C. Milot, J.M. Tobin, Metal-anion sorption by chitosan beads: Equilibrium and kinetic studies, Ind. Eng. Chem. Res. 37(4) (1998) 1454–1463.
[24] K.P. Raven, A. Jain, R.H. Loeppert, Arsenite and arsenate adsorption on ferrihydrite: Kinetics, equilibrium, and adsorption envelopes, Environ. Sci. Technol. 32(3) (1998) 344–349.

[25] C. Chang, W. Tsai, C. Chang, Adsorption of polyethylene glycol (PEG) from aqueous solution onto hydrophobic zeolite, J. Colloid Interface Sci. 260(2) (2003) 273–279.
[26] M.Y. Chang, R.S. Juang, Adsorption of tannic acid, humic acid, and dyes from water using the composite of chitosan and activated clay, J. Colloid Interface Sci. 278(1) (2004) 18–25.
[27] A. Özcan, E. Öncü, A.S. Özcan, Kinetics, isotherm and thermodynamic studies of adsorption of Acid Blue 193 from aqueous solutions onto natural sepiolite, Colloids Surf. A 277(1) (2006) 90–97.
[28] A. Safa Özcan, B. Erdem, A. Özcan, Adsorption of acid blue 193 from aqueous solutions onto Na-bentonite and DTMA-bentonite, J. Colloid Interface Sci. 280(1) (2004) 44–54.
[29] F.C. Wu, R.L. Tseng, R.S. Juang, Kinetic modeling of liquid-phase adsorption of reactive dyes and metal ions on chitosan, Water Res. 35(3) (2001) 613–618.
[30] X. Yang, B. Al-Duri, Kinetic modeling of liquid-phase adsorption of reactive dyes on activated carbon, J. Colloid Interface Sci. 287(1) (2005) 25–34.
[31] L. Chan, W. Cheung, G. McKay, Adsorption of acid dyes by bamboo derived activated carbon, Desalin. 218(1) (2008) 304–312.
[32] G. McKay et al., Adsorption of reactive dye from aqueous solutions by compost, Desalin. Water Treat. 28(1–3) (2011) 164–173.
[33] E.L.K. Mui, W. Cheung, G. McKay, Tyre char preparation from waste tyre rubber for dye removal from effluents, J. Hazard. Mater. 175(1) (2010) 151–158.
[34] D.M. Ruthven, Principles of Adsorption and Adsorption Processes. Wiley Publication, New York, NY, 1984.
[35] J. Crank, The Mathematics of Diffusion, Oxford Science Publication, London, 1979.
[36] I. Langmuir, The constitution and fundamental properties of solids and liquids. part I. solids, J. Am. Chem. Soc. 38(11) (1916) 2221–2295.
[37] I. Langmuir, The adsorption of gases on plane surfaces of glass, mica and platinum, J. Am. Chem. Soc. 40(9) (1918) 1361–1403.
[38] H. Freundlich, Over the adsorption in solution, J. phys. Chem. 57 (1906) 385–470.
[39] L. Jossens et al., Thermodynamics of multi-solute adsorption from dilute aqueous solutions, Chem. Eng. Sci. 33(8) (1978) 1097–1106.
[40] J.C. Morris, W. Weber, Removal of biologically-resistant pollutants from waste waters by adsorption, in Advances in Water Pollution Research, Proceeding of the 1 st International Conference on Water Pollution Research, Pergamon Press, New York. 1962.
[41] G. McKay, V.J.P. Poots, Kinetics and diffusion processes in colour removal from effluent using wood as an adsorbent, J. Chem. Technol. Biotechnol. 30(1) (1980) 279–292.